

# Effect of nano-particle addition on grain structure evolution of friction stir processed Al 6061 during post-weld annealing

Guo Junfeng<sup>1\*</sup>, Lee Bing Yang<sup>1</sup>, Du Zhenglin<sup>2</sup>, Bi Guijun<sup>1</sup>, Tan Ming Jen<sup>2</sup>, Wei Jun<sup>1</sup>

<sup>1</sup>Singapore Institute of Manufacturing Technology  
71 Nanyang Drive, Singapore 638075

<sup>2</sup>Nanyang Technological University, 50 Nanyang Avenue, Singapore 639798

\*Corresponding author: Dr Guo Junfeng, Email: [jfguo@simtech.a-star.edu.sg](mailto:jfguo@simtech.a-star.edu.sg)

Keywords: Friction stir processing; Nano-composites; Grain structure; Abnormal grain growth

## Abstract

The fabrication of nano-composites is quite challenging because uniform dispersion of nano-sized reinforcements in metallic substrate is difficult to achieve using powder metallurgy or liquid processing methods. In the present study, Al-based nano-composites reinforced with Al<sub>2</sub>O<sub>3</sub> particles have been successfully fabricated using friction stir processing. The effects of nano-Al<sub>2</sub>O<sub>3</sub> particle addition on grain structure evolution of friction stir processed Al matrix during post-weld annealing were investigated. It was revealed that the pinning effect of Al<sub>2</sub>O<sub>3</sub> particles retarded grain growth and completely prevented abnormal grain growth during post weld annealing at 470 °C. However, abnormal grain growth can still occur when the composite material was annealed at 530 °C. The mechanism involved in the grain structure evolution and the effect of nano-sized particle addition on the mechanical properties was discussed therein.

## 1. Introduction

It has been reported that abnormal grain growth (AGG) could occur during the post weld heat treatment (PWHT) of friction stir welds. Abnormal grain growth alternatively known as secondary recrystallization, takes place in recrystallized materials at high temperatures during annealing. This process may lead to the formation of large grains of even greater than several millimeters [1], which causes negative effects for mechanical property, especially the formability of material. A review of this phenomenon in friction stir welded joints could be found in the work of Y.S. Sato et al. [2]. Kh.A.A. Hassan et al. [3] studied the stability of friction stir welded AA7010 alloy during solution treatment. It was concluded that the abnormal grain growth might be promoted by the fine grain structure in nugget zone and the partial dissolution of second phase particles during solution treatment. It was also revealed that the rotation speed and the welding speed can be used as a tool to control abnormal grain growth during subsequent heat treatment [4]. According to Humphreys [5], an obvious and effective solution to prevent abnormal grain growth would be to increase the particle pinning pressure by increasing the density of stable second phase particles (increase the ratio of  $F_v/d$ , where  $F_v$  is the volume fraction of second phase particle and  $d$  is the particle diameter). However, addition of such fine particles into metal matrix is quite challenging because uniform dispersion of nano-sized reinforcements in metallic substrate is difficult to achieve by using conventional powder metallurgy or liquid processing methods [6, 7]. Over past few years, friction stir processing (FSP) method has attracted much attention since the first attempt on fabrication of nano-particles reinforced metal matrix composites (MMC) [8].

Friction stir processing, a relatively new processing technique, was developed for microstructural modification based on the basic principles of friction stir welding (FSW) [9, 10]. Similar to friction stir welding, FSP is carried out by using a rotating non-consumable tool plunging into the workpiece. The heat generated by the friction between welding tool and workpiece will plasticize the material, but the workpiece never melts. A volume of material can then be processed as the tool travels forwards. The concept of fabricating MMCs by FSP is considered to be beneficial as undesirable intermetallics formation between reinforcement and matrix can be avoided [11, 12]. Our previous work showed that multi-pass FSP could uniformly disperse nano-sized particles into aluminum matrix.

More pronounced grain refinement and significant increases in microhardness and tensile strengths were observed in comparison with the Al matrix in the same condition. Nonetheless, the effects of nano-particles addition on grain structure evolution of friction stir processed Al matrix during post-weld annealing has yet been reported. The present study aims to investigate the pinning behavior of Al<sub>2</sub>O<sub>3</sub> particles during post-weld annealing of friction stir processed Al matrix. The grain structures of the friction stir processed Al without/with particle addition were compared before/after annealing.

## 2. Experimental Procedures

Rolled plates of AA6061 alloy and nano-sized Al<sub>2</sub>O<sub>3</sub> particles (nominal diameter: 320 nm) were used as base materials. The Al plates were cut into dimensions measuring 300 mm long and 100 mm wide (rolling direction). An array of 960 cylindrical holes measuring 1 mm in diameter, 2 mm in depth was machined in an area of 240 mm x 50 mm as reservoir to hold the Al<sub>2</sub>O<sub>3</sub> particles for FSP. All plates were then carefully degreased with acetone and dried in air. Alumina slurry with a concentration of 50 vol.% was prepared by step-wise addition of alumina nano-powder (Sumitomo-AKP30, Japan) to deionized water during ball milling. 0.5wt% Dolapix CE64 (Zschimmer & Schwarz, Germany) was added as a dispersant. The prepared slurry was squeezed into the holes in aluminum plates and dried in a convection oven at 110 °C for 2 h. The density of the dried slurry in the holes was estimated to be 2.189 g/cm<sup>3</sup>. The nominal volume fraction of the reinforcement in the composite produced by FSP is around 14%. However, the actual particle concentration could be slightly lower than this value because of the particle loss during FSP ( $F_v = 0.12$  will be used for later calculations).

Friction stir processing is carried out using a robotic friction stir welding machine (Friction Stir Link, ABB IRB7600 Robot) which is capable of generating up to 12 kN downward force. The welding tool has a shoulder with 12.5 mm diameter and a threaded conical probe with three flats (2 mm probe length and 5 mm diameter at probe base). In order to uniformly disperse nano-particles in the matrix, four passes FSP tests were conducted at a rotation speed of 1200 rpm, travel speed of 3 mm/s, tilt angle of 2.5° and downward force of 3.6-4.2 kN. The friction stir processed specimens were then annealed at 470 °C and 530 °C respectively for one hour.

Metallographic samples were transversely sectioned from the specimens and polished using conventional mechanical polishing method. Microstructural characterization was performed using a scanning electron microscope (EVO-50 & ULTRA plus, Carl Zeiss) equipped with electron backscattered diffraction (EBSD). For EBSD analysis, a further electro-polishing after mechanical polishing was carried out using a mixture of 80% alcoholic and 20% HClO<sub>4</sub> for 5-20 s at ambient temperature. The voltage during electro-polishing was fixed at 15 V while the current was not controlled. Step size between 0.2-1 μm was used during data acquisition.

## 3. Results & Discussion

### 3.1 Microstructures before annealing

Fig. 1 shows the SEM images of the base metal and the friction stir processed Al without/with Al<sub>2</sub>O<sub>3</sub> particle addition. Some Al-Fe containing intermetallics scatter in the base metal (Fig. 1a). Invisible change is observed after FSP though it is believed that FSP might have redistributed these intermetallics. As seen in Fig. 1c, uniform dispersion of Al<sub>2</sub>O<sub>3</sub> particle (white color) was obtained through multi-pass FSP.

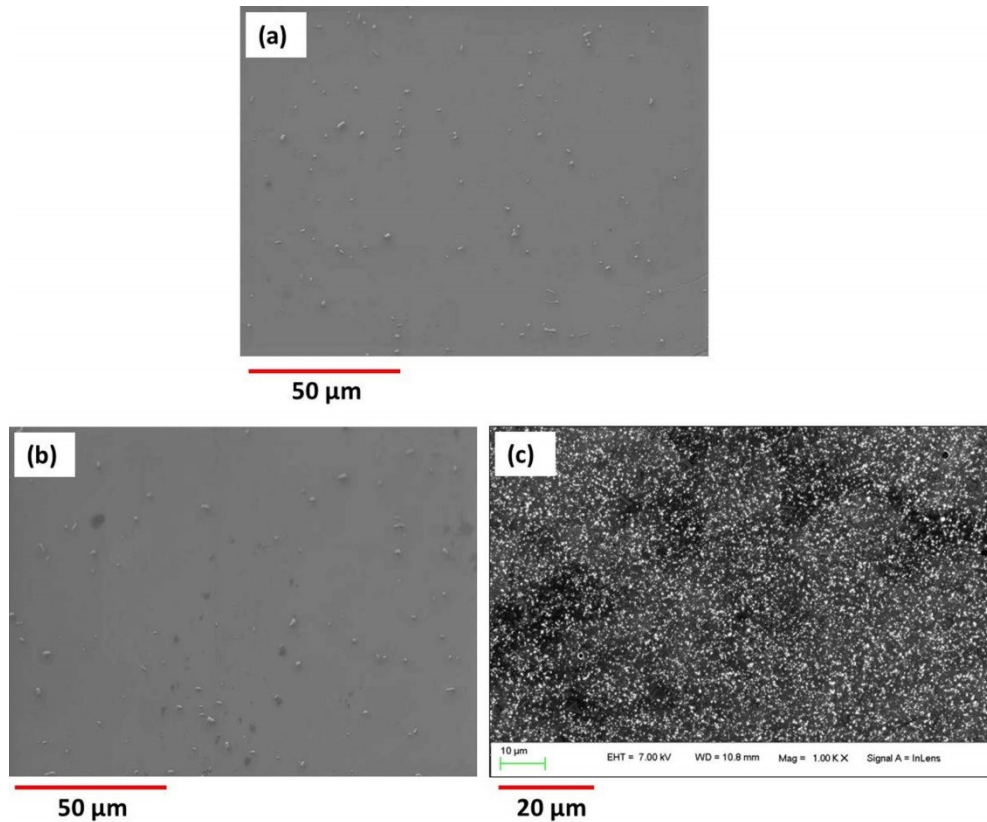


Fig. 1 SEM images of (a) the base metal, (b) the friction stir processed Al, and (c) friction stir processed Al with  $\text{Al}_2\text{O}_3$  particle addition.

The grain structure of the base metal and the friction stir processed Al without/with  $\text{Al}_2\text{O}_3$  particle addition is shown in Fig. 2. Significant grain refinement was observed in the friction stir processed specimens as compared to that of base metal. The equivalent grain size diameters were obtained through EBSD analysis over around 1000 grains with grain boundary angle larger than  $15^\circ$ . The average grain size in the base metal and the friction stir processed Al without/with  $\text{Al}_2\text{O}_3$  particle addition are  $70 \pm 3 \mu\text{m}$ ,  $5.9 \pm 0.2 \mu\text{m}$ ,  $2.5 \pm 0.1 \mu\text{m}$  respectively. This grain refinement can be attributed to continuous dynamic recrystallization in which a continuous introduction of strain is coupled with rapid recovery and migration of subgrain/grain boundaries. It is worth noting that more pronounced reduction in grain size was characterized in the specimen with  $\text{Al}_2\text{O}_3$  particle addition. The large amount of nano-sized  $\text{Al}_2\text{O}_3$  particles acted as nucleation sites during dynamic recrystallization and thus promoted formation of new grains. In addition, some of these  $\text{Al}_2\text{O}_3$  particles might also exert strong pinning pressure to the grain boundaries and limit grain growth. The grain boundary misorientation distribution for the friction stir processed Al without/with  $\text{Al}_2\text{O}_3$  particle addition is shown in Fig. 3. The specimen with particle addition contains much higher fraction of low angle grain boundaries. It was suggested by Tweed et al. [13] that the interaction between the pinning particles and grain boundaries is very complicated. In their study, a relatively high fraction of high angle boundaries were found to be unpinned, all the low angle boundaries analyzed were found to exhibit pinning interactions. This is probably the reason why in the present study, the number of low-angle boundaries ( $\leq 15^\circ$ ) increased significantly with the addition of alumina particles. For high angle grain boundaries, the high energy of such type grain boundary could curve the boundary plane when it touches a second phase inclusion, which allows bypassing long before the boundary as a whole is bent into a half circle. In contrast, the lower energy and higher flexibility of a low angle grain boundary leads to a more perturbed boundary plane. The process of migration of a low angle grain boundary is a cooperative process relying on the sequential movement of the constituent dislocations.

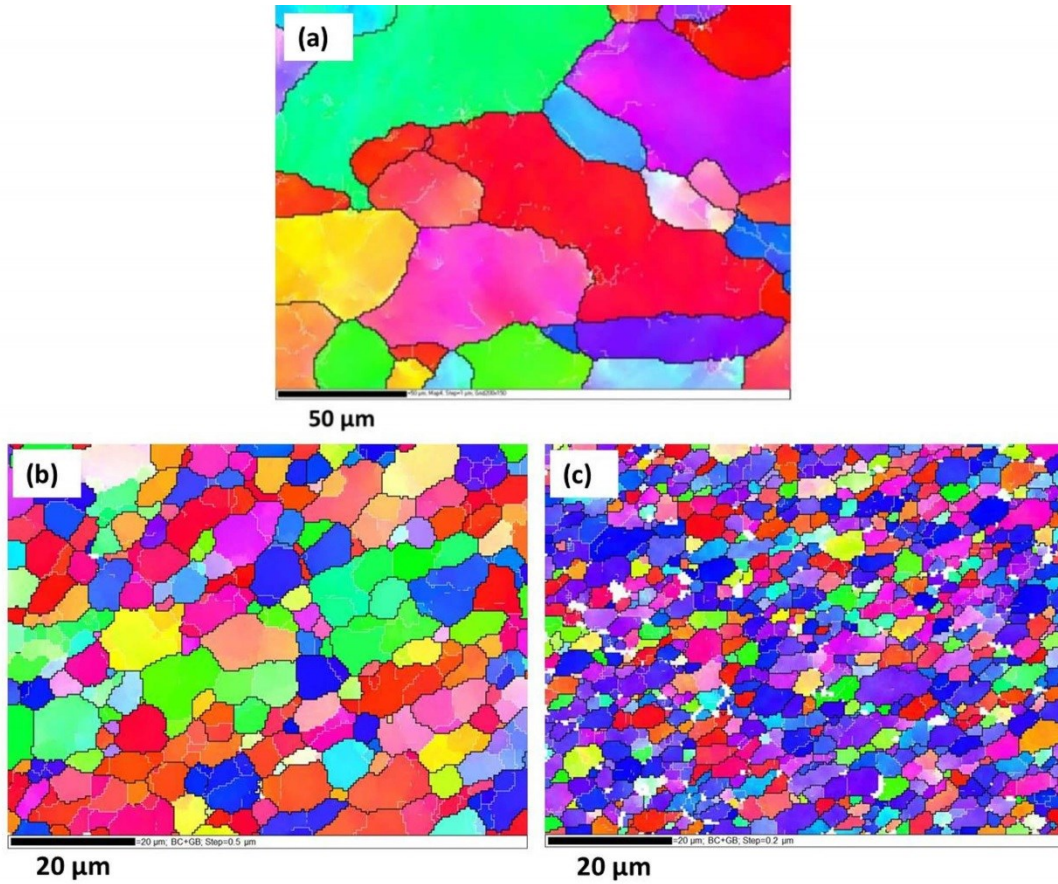


Fig. 2 Grain structure of (a) the base metal, (b) the friction stir processed Al, and (c) friction stir processed Al with Al<sub>2</sub>O<sub>3</sub> particles addition.

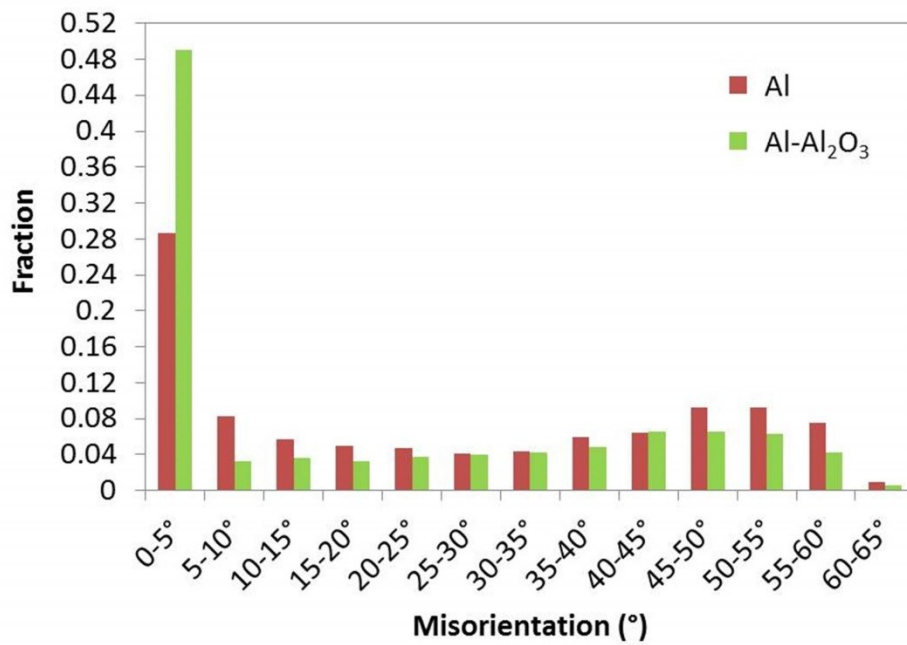


Fig. 3 Grain boundary misorientation distribution for the friction stir processed Al without/with Al<sub>2</sub>O<sub>3</sub> particle addition

### 3.2 Microhardness & tensile testing

The Vicker's microhardness values measured in the friction stir processed materials are listed in Table 1. The increase in the friction stir processed Al alloy is mainly due to the grain refinement and solution treatment effect induced by FSP thermal cycle, whereas the further increase in the Al-Al<sub>2</sub>O<sub>3</sub> composites produced by FSP can be attributed to the much finer grain size and the Orowan strengthening due to addition of finely dispersed nano-Al<sub>2</sub>O<sub>3</sub> particles.

Table 1 Microhardness values measured in the base metal and friction stir processed materials

Materials	AA6061-O	FSPed Al	Al-Al <sub>2</sub> O <sub>3</sub> Composites
HV <sub>0.05</sub>	55±3	75±2	103±2

The tensile properties of Al and Al-Al<sub>2</sub>O<sub>3</sub> composites produced by FSP are listed in Table 2. The tensile strengths of Al after FSP increased significantly compared with the annealed base metal. This is mainly due to the grain refinement (Fig. 2) and solution treatment effect induced by FSP thermal cycle. With Al<sub>2</sub>O<sub>3</sub> particle addition, the tensile strengths further increased marginally, especially for the ultimate tensile strength (UTS). It is believed that the solution treatment effect induced by FSP thermal cycle is similar to that without particle addition. Therefore, this further increase of tensile strengths is attributed to the grain structure difference and the Orowan strengthening due to addition of finely dispersed nano-Al<sub>2</sub>O<sub>3</sub> particles.

Table 2 Tensile properties of Al base metal and Al-Al<sub>2</sub>O<sub>3</sub> composites produced by FSP

Materials	UTS (MPa)	YS (MPa)	Elongation (%)	E (GPa)
AA6061-O*	125	55	25	69
FSPed Al	195±3	95±4	18±2	72±1
Al-Al <sub>2</sub> O <sub>3</sub> Composites	228±5	111±3	24±1	76±3

\*Tensile property values for AA6061-O base metal are from ASM Handbook

### 3.3 Microstructures after annealing

The friction stir processed Al specimens without/with Al<sub>2</sub>O<sub>3</sub> particle addition were then annealed at 470 °C and 530 °C using an air furnace. The heat treatment at 470 °C and 530 °C are most commonly used as solution treatment temperature for Al alloys. Both specimens showed similar morphology under SEM compared to those of specimens before annealing (Fig. 1b & c). The grain structures however changed drastically, as shown in Fig. 4. For specimens annealed at 470 °C, the friction stir processed Al specimen without Al<sub>2</sub>O<sub>3</sub> particle exhibited abnormal grain growth, as shown in Fig. 4a. Large grains with equivalent diameter up to 1 mm can be observed. Such abnormal grain growth is mainly driven by the stored energy in the drastically deformed fine grain boundaries. It is interesting to note that the friction stir processed Al specimen with Al<sub>2</sub>O<sub>3</sub> particles only showed slight growth to around 3-4 μm although their initial grains were actually finer than the specimen without particle (Fig. 4b). This is mainly attributed to the pinning pressure of large amount of Al<sub>2</sub>O<sub>3</sub> particles has stopped grain boundary migration although the driving force of the initial grains is higher than the specimen without Al<sub>2</sub>O<sub>3</sub> particles. In contrast, for specimens annealed at 530 °C, both specimens without/with Al<sub>2</sub>O<sub>3</sub> particles showed abnormal grain growth in the friction stir processed zone as shown in Figs. 4c & 4d. At high annealing temperatures, the energy of grains boundaries increased tremendously. Thus the grains boundaries could pass the pinning particles very easily as the effectiveness of particle pinning have decreased substantially.

According to Humphreys [1,5], stable second phase particles may exert a pinning effect during grain boundary migration and thus prevent the occurrence of abnormal grain growth. In a cellular microstructure containing second phase particles, abnormal grain growth will occur if an individual cell grows faster than the surrounding matrix of average cells, which can be described as

$$\bar{R} \frac{dR}{dt} - R \frac{d\bar{R}}{dt} > 0 \quad (1)$$

Where  $R$ ,  $\bar{R}$ ,  $dR/dt$  and  $d\bar{R}/dt$  are the cell radius and the growth rates of the cell and the surrounding average cells.

$$\frac{dR}{dt} = M \left( \frac{\bar{\gamma}}{\bar{R}} - \frac{\gamma}{R} - \frac{3F_v \gamma}{d} \right) \quad (2)$$

$$\frac{d\bar{R}}{dt} = \bar{M} \bar{\gamma} \left( \frac{1}{4\bar{R}} - \frac{3F_v}{d} \right) \quad (3)$$

Where  $\gamma$  and  $\bar{\gamma}$  are the boundary energies of the individual and average matrix cells. In a friction stir processed zone,  $\bar{\gamma} = \gamma$ , normal grain growth of the matrix will stagnate when  $d\bar{R}/dt = 0$ . Under such conditions, abnormal grain growth of an individual grain can still occur provided it has a sufficient size differential ( $X = R/\bar{R}$ ) over its surrounding neighbors, which gives

$$\bar{R} \frac{dR}{dt} > 0 \quad (4)$$

Rearrangement of (2) and (4) gives

$$\bar{R} < \frac{d}{3F_v} \left( 1 - \frac{1}{X} \right) \quad (5)$$

Where  $d$  is the equivalent particle size diameter. In the present study,  $d = 0.32$ ,  $F_v = 0.12$ , the maximum  $X = 5$  (as measured by EBSD analysis), abnormal grain growth will easily occur as long as  $\bar{R} < 0.7 \mu\text{m}$ . Obviously, the  $\text{Al}_2\text{O}_3$  particles added in the matrix can provide sufficient pinning pressure to stop abnormal grain growth under relatively low annealing temperatures. However, at high annealing temperatures, the effectiveness of particle pinning has decreased substantially, which increases the critical  $\bar{R}$  tremendously and makes abnormal grain growth possible.

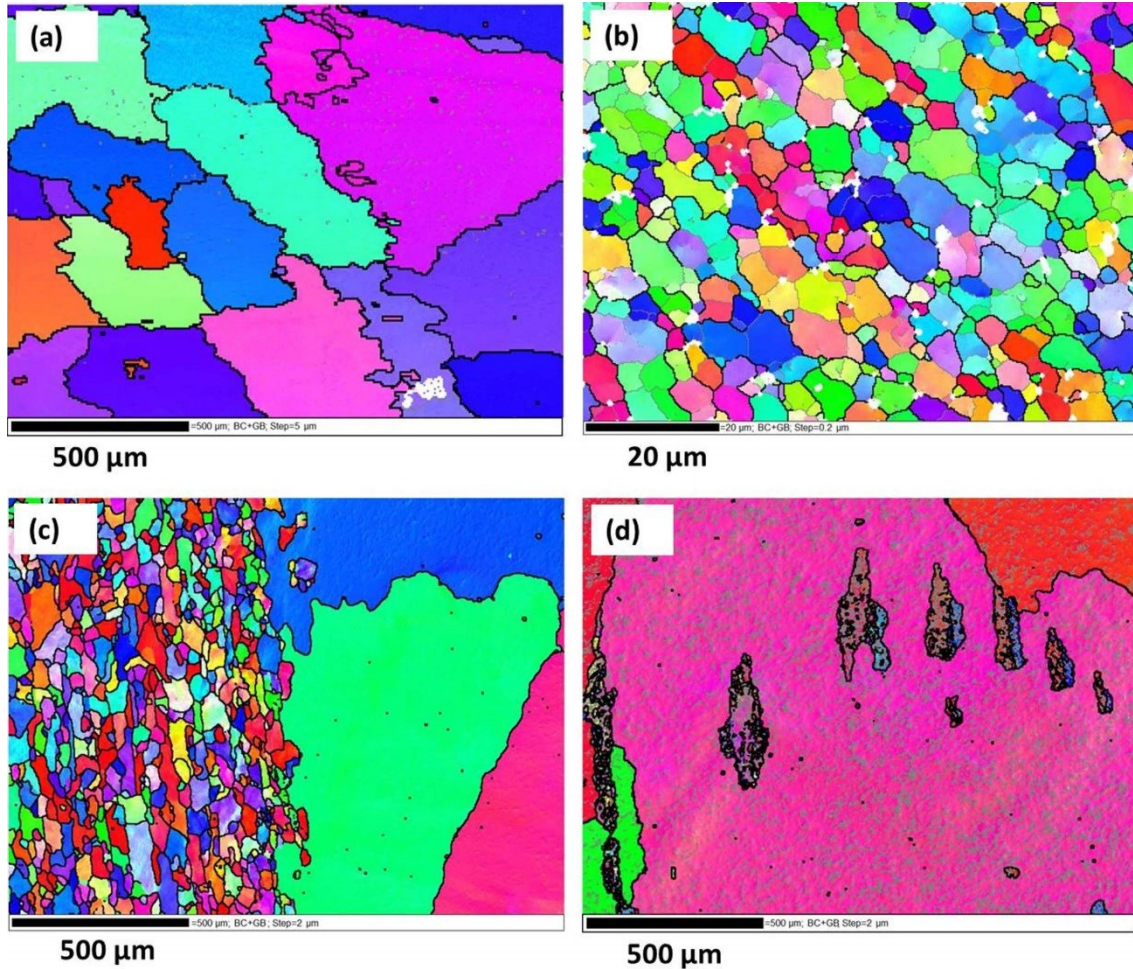


Fig. 4 Grain structure of the friction stir processed specimens heat treated at (a) 470 °C without particle, (b) 470 °C with  $\text{Al}_2\text{O}_3$  particle, (c) 530 °C without particle, (d) 530 °C with  $\text{Al}_2\text{O}_3$  particle addition.

#### 4. Conclusions

In the present study, the effects of nano- $\text{Al}_2\text{O}_3$  particle addition on grain structure evolution of friction stir processed Al matrix during post-weld annealing were investigated. The following conclusions can be drawn based on the above results and discussion.

- Uniform dispersion of  $\text{Al}_2\text{O}_3$  particles (white color) was obtained through multi-pass FSP;
- Addition of  $\text{Al}_2\text{O}_3$  particles exerted strong pinning pressure to the grain boundary and thus led to more pronounced grain size reduction;
- The pinning effect of  $\text{Al}_2\text{O}_3$  particles completely prevented abnormal grain growth during post weld annealing at 470 °C. However, the effectiveness of the pinning decreased substantially and abnormal grain growth can still occur at 530 °C.
- The microhardness and tensile strengths of the composites increased significantly with the addition of nano-sized  $\text{Al}_2\text{O}_3$  particles while maintaining comparable elongation values. The increases are mainly attributed to grain refinement and Orowan strengthening effect induced by the finely dispersed  $\text{Al}_2\text{O}_3$  particles.

## 5. References

- [1] F.J. Humphreys and M. Hatherly, Recrystallization and Related Annealing Phenomena, 2nd ed. (Oxford, OX: Elsevier Ltd., 2004), pp. 321-328.
- [2] Y.S. Sato, H. Watanabe and H. Kokawa, : Sci. Technol. Weld. Joining, 12, 318 (2007).
- [3] Kh. A.A. Hassan, A.F. Norman, D.A. Price and P.B. Prangnell, : Acta Mater., 51, 1923 (2003).
- [4] M.M. Attallah and H.G. Salem, : Mater. Sci. Eng., A391, 51 (2005).
- [5] F.J. Humphreys, : Acta Mater., 45, 5031(1997).
- [6] N. Chawla, K.K. Chawla, Metal Matrix Composites, (New York, NY: Springer, 2006), pp. 31-55.
- [7] S.R. Bakshi, D. Lahiri, A. Agarwal, : Int. Mater. Rev., 55, 41 (2011).
- [8] R.S. Mishra, Z.Y. Ma, I. Charit, : Mater. Sci. Eng., A341, 307 (2003).
- [9] R.S. Mishra, Z.Y. Ma, Mater. Sci. Eng., R50, 1 (2005).
- [10] Z.Y. Ma, Metall. Mater. Trans. A, 39A, 642 (2008).
- [11] J. Guo, P. Gougeon, X.-G. Chen, Mater. Sci. Eng., A553, 149 (2012).
- [12] E.R.I. Mahmoud, M. Takahashi, T. Shibayanagi, K. Ikeuchi, Wear, 268, 1111 (2010).
- [13] C.J. Tweed, B. Ralph, N. Hansen, Acta Metall., 32, 1407 (1984).